

Protograph-Based LDPC Code Design for Probabilistic Shaping with On-Off Keying

Alexandru Dominic Git[†], Balázs Matuz[†], Fabian Steiner[‡]

[†]Institute of Communications and Navigation, German Aerospace Center (DLR), Germany

[‡]Institute for Communications Engineering, Technical University of Munich, Germany

Email: a.git@tum.de, balazs.matuz@dlr.de, fabian.steiner@tum.de

Abstract—This work investigates protograph-based low-density parity-check (LDPC) codes for the additive white Gaussian noise (AWGN) channel with on-off keying (OOK) modulation. A non-uniform distribution of the OOK modulation symbols is considered to improve the power efficiency especially for low signal-to-noise ratios (SNRs). To this end, a specific transmitter architecture based on time sharing is proposed that allows probabilistic shaping of (some) OOK modulation symbols. Tailored protograph-based LDPC code designs outperform standard schemes with uniform signaling and off-the-shelf codes by 1.1 dB for a transmission rate of 0.25 bits/channel use.

I. INTRODUCTION

Free-space optical (FSO) communication has numerous advantages: large bandwidth, license free spectrum, high data rate, and easy deployment. Intensity modulation (IM) schemes, such as on-off keying (OOK) and pulse-position modulation (PPM) are widely used for direct detection (DD) receivers [1, Sec. V], since they do not require an optical phase-locked loop to track the carrier phase at the receiver. Non-coherent schemes are currently considered for deep-space communications, near earth communications and space-to-ground communications [2]–[4].

We study average power constrained additive white Gaussian noise (AWGN) channels with low transmission power. For such channels, OOK with a uniform distribution on the two levels shows a significant loss compared to optimal signaling using a non-uniform distribution. We can generate a non-uniform distribution by using PPM. However, PPM requires symbol metric decoding (SMD) for good performance, i.e., the forward error correction (FEC) decoder must operate on the whole PPM symbol. Instead, if binary codes with bit-metric decoding (BMD) are considered, bit-wise soft-information is obtained by marginalizing over the bit-levels of the PPM symbols and their correlation is not exploited, which generally leads to a performance loss. While this loss is small for some modulation schemes with a proper choice of the binary labeling (e.g., quadrature amplitude modulation (QAM) with a binary reflected Gray code (BRGC) [5]), BMD with PPM experiences significant losses with respect to channel capacity [6]. This is illustrated in Fig. 1, where a gap of almost 1.7 dB between OOK with a capacity achieving input distribution and 8-PPM with BMD at a rate of 0.2 bits per channel use (bpcu) is visible. To reduce this gap, iterations between the decoder and the demodulator have been considered [6] but this increases receiver complexity.

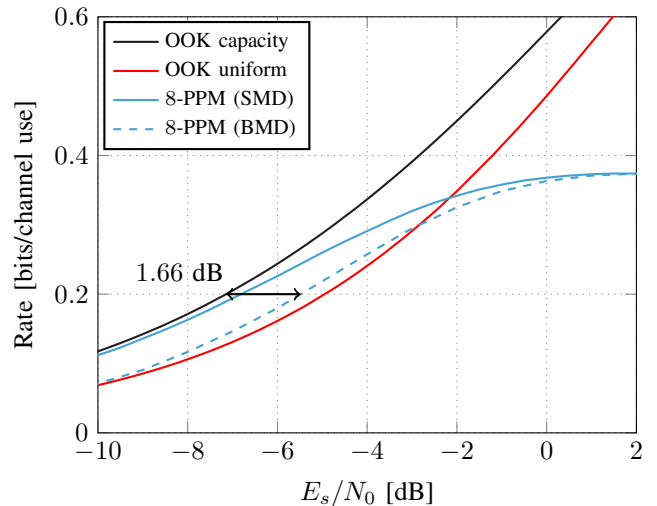


Fig. 1. Achievable rates for OOK and PPM.

In general, the combination of probabilistic shaping (PS) with FEC is challenging as conventional schemes (e.g., [7, Sec. 6.2], [8]) place the shaping operation after FEC encoding so that it needs to be reversed before (or performed jointly with) the FEC decoding. This is prone to error propagation, synchronization issues [9, Sec. IV-A] or requires a joint and thus inflexible shaping/FEC code design. Recently, probabilistic amplitude shaping (PAS) was proposed, which avoids these difficulties by *reverse concatenation* [10]. PAS exploits the symmetry of the capacity achieving input distribution, but PAS cannot be used for OOK, as the optimal input distribution is not symmetric around the origin. Following the idea of *sparse-dense* transmission [11], we propose a time sharing (TS) scheme which combines non-uniform signaling for OOK with FEC. Using a binary FEC code of block length n and code rate R_C with systematic encoding, a number of $R_C \cdot n$ OOK symbols is transmitted with a non-uniform distribution, while the remaining $(1 - R_C) \cdot n$ parity bits are sent with a uniform distribution. A similar approach for coherent higher order modulations with non-binary low-density parity-check (LDPC) codes was suggested in [12], while binary codes were investigated for a nonlinear Fourier transform based, optical transmission system in [13] without a tailored LDPC code design.

In this work, we describe a PS approach for the average power constrained AWGN channel with OOK modulation via TS and calculate achievable rates for this signaling strategy. We distinguish two cases. In the first one, both shaped and uniform symbols have the same amplitude. In the second case, the amplitudes may be chosen differently allowing an additional degree of freedom. For the protograph-based low-density parity-check (P-LDPC) code design, we use extrinsic information transfer (EXIT) analysis with the surrogate approach of [14]. The proposed PS scheme yields gains of up to 1.1 dB with respect to uniform OOK and off-the-shelf DVB-S2 codes [15].

II. SYSTEM MODEL AND OPTIMAL SIGNALING FOR OOK

Consider transmission over an average power constrained AWGN channel with

$$Y = X + N$$

for n channel uses. The Gaussian noise N has zero mean and variance σ^2 . The OOK constellation symbols X are from the binary set $\mathcal{X} = \{0, A\}$. The average power constraint is $\mathbb{E}[X^2] \leq P$, where

$$\mathbb{E}[X^2] = A^2 P_X(A). \quad (1)$$

Without loss of generality, let $P = 1$. We define the signal-to-noise ratio (SNR) as $E_s/N_0 = 1/(2\sigma^2)$.

An achievable rate is given by the mutual information $I(X; Y)$ and the maximum achievable rate is the solution to the following optimization problem

$$C = \max_{P_X} I(X; Y) \quad \text{subject to} \quad A^2 P_X(A) \leq 1. \quad (2)$$

We refer to (2) as the ‘‘OOK capacity’’, which is shown in Fig. 1. Note that the inequality constraint of the average power constraint is always active, so that the amplitude is $A = \sqrt{1/P_X(A)}$. If a uniform distribution is chosen, i.e., $P_X(0) = P_X(A) = 0.5$, we observe a significant degradation in power efficiency.

III. PROBABILISTIC SHAPING VIA TIME SHARING

We use a linear FEC code of dimension k and block length n . The code rate is $R_C = k/n$. Its systematic generator matrix is of form $\mathbf{G} = (\mathbf{I} \mathbf{P})$, where \mathbf{I} is the $k \times k$ identity matrix and \mathbf{P} is the $k \times (n - k)$ parity forming part. For encoding, the length k information vector $\mathbf{u} \in \{0, 1\}^k$ is multiplied with \mathbf{G} yielding the codeword $\mathbf{c} = (\mathbf{u} \mathbf{p})$ with $\mathbf{p} = \mathbf{u}\mathbf{P}$. The parity bits \mathbf{p} are approximately uniformly distributed, since they are the result of a modulo-2 sum of many information bits (see [16, Sec. IV-A] for details). In contrast, the distribution of the information bits can be chosen at will, as explained later. This observation gives rise to a TS sharing scheme which has been named *sparse-dense* transmission in [11], [17].

In the following, we distinguish between a modulated information symbol X_S and modulated parity symbol X_U . We have $P_{X_S} = (p_0 \ p_1)$ and $P_{X_U} \approx (0.5 \ 0.5)$. For the information part, i.e., for a number of $R_C n$ channel uses, we use the signaling

set $\mathcal{X}_S = \{0, A_S\}$. For the remaining $(1 - R_C)n$ channel uses involving the parity bits, the signaling set $\mathcal{X}_U = \{0, A_U\}$.

A constant-composition distribution matcher (CCDM) is used to realize the non-uniformly distributed symbols [18]. The CCDM encodes k' uniformly distributed bits into a length k shaped information bit sequence \mathbf{u} which is then FEC encoded. The distribution matcher (DM) is characterized by its matching rate

$$R_{DM} = \frac{k'}{k}. \quad (3)$$

For long k the DM rate (3) approaches the entropy of the output distribution [18]. Therefore, we may write $R_{DM} = H(X_S)$ for large k and the overall transmission rate is

$$R_{TX} = H(X_S) \cdot R_C. \quad (4)$$

Thus R_{TX} is directly related to $P_{X_S}(A_S) = p_1$ via

$$p_1 = H^{-1}\left(\frac{R_{TX}}{R_C}\right). \quad (5)$$

For the general signaling set \mathcal{X} , the receiver performs soft-demapping and calculates the soft-information values

$$L = \underbrace{\log\left(\frac{p_{Y|X}(y|A)}{p_{Y|X}(y|0)}\right)}_{\text{channel LLR}} + \underbrace{\log\left(\frac{P_X(A)}{P_X(0)}\right)}_{\text{prior}}. \quad (6)$$

Note that the prior term is zero for the parity bits. The soft-information serves as an input to an LDPC decoder which performs belief propagation decoding. The system setup is depicted in Fig. 2.

IV. RATES FOR THE TIME SHARING SCHEME

A. Transmission Rate

An achievable rate of the TS scheme is given by

$$R_{TS} = R_C I(X_S; Y_S) + (1 - R_C) I(X_U; Y_U). \quad (7)$$

From (4), reliable communication is guaranteed as long as $R_{TX} \leq R_{TS}$. In the following, we distinguish two cases.

B. Case 1: Same Pulse Amplitudes

Consider the case where both pulse amplitudes are the same, i.e., $A_S = A_U = A$. The average power constraint (1) is

$$\mathbb{E}[R_C X_S^2 + (1 - R_C) X_U^2] = \left(R_C p_1 + (1 - R_C) \frac{1}{2}\right) A^2 \quad (8)$$

and the optimization problem for (7) is

$$R_{TS1}^* = \max_{p_1, A} R_{TS} \quad \text{subject to} \quad \left(R_C p_1 + (1 - R_C) \frac{1}{2}\right) A^2 \leq 1. \quad (9)$$

As for (2), the power constraint is always active. Thus, for a fixed p_1 we have $A = 1/\sqrt{R_C p_1 + (1 - R_C)/2}$.

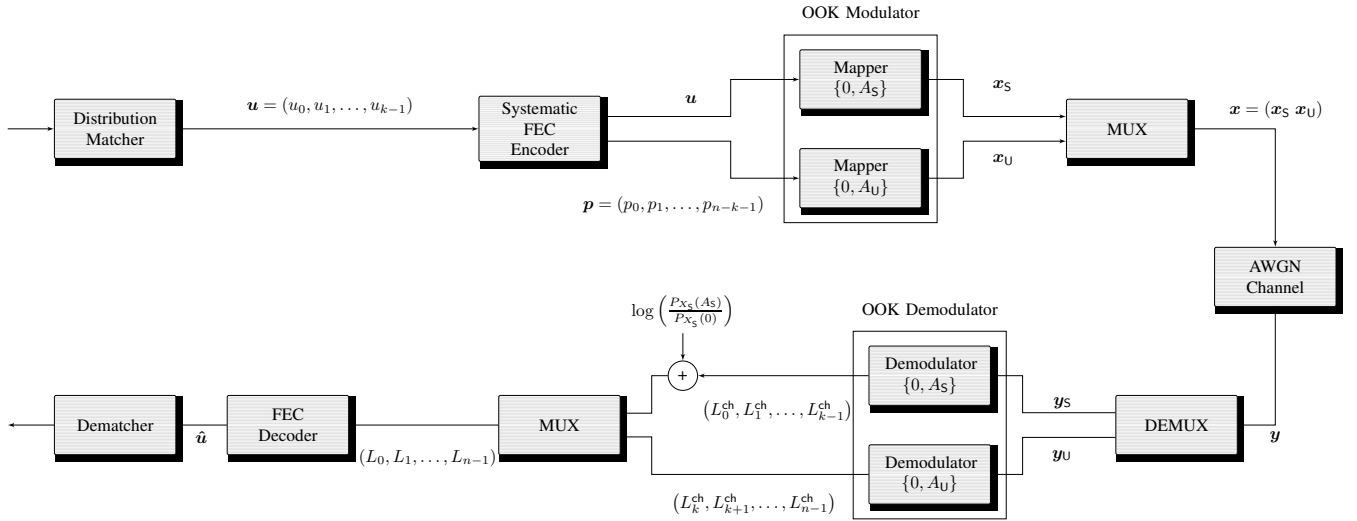


Fig. 2. Block diagram of the proposed TS transceiver architecture for probabilistic shaping with OOK.

C. Case 2: Individual Pulse Amplitudes

We now permit different pulse amplitudes A_S and A_U . The power constraint (1) becomes

$$\mathbb{E} [R_C X_S^2 + (1 - R_C) X_U^2] = R_C p_1 A_S^2 + (1 - R_C) \frac{1}{2} A_U^2.$$

Similar to the first case, we have

$$R_{TS_2}^* = \max_{p_1, A_S, A_U} R_{TS}$$

$$\text{subject to } R_C p_1 A_S^2 + (1 - R_C) \frac{1}{2} A_U^2 \leq 1. \quad (10)$$

Again, the average power constraint is always active. Thus, for a given p_1 the amplitude A_U is given by $A_U = \sqrt{(1 - R_C p_1 A_S^2) / ((1 - R_C) / 2)}$, where A_S is subject to optimization.

D. Numerical Comparison of Both Cases

We plot the achievable rates for both time sharing schemes in Fig. 3 for the code rates $R_C = 0.5$ and $R_C = 0.75$. The dashed curves show the transmission rates (4) with the optimized pulse probability p_1 according to (9) and (10). The crossing of the R_{TS} and R_{TX} curves indicates the optimal operating points for the chosen code rates. Comparing (2) and (7), we observe that using a low code rate, i.e., $R_C = 0.5$ in Fig. 3, increases the gap as the fraction of transmission symbols with a uniform distribution also increases with lower R_C . The gap to the OOK capacity is about 1.0 dB for $R_C = 0.5$, while it reduces to 0.3 dB for $R_C = 0.75$ code. These results motivate using a high rate code, even for low transmission rates. This requires using a pulse probability different from the optimal one from (9) or (10). However, it provides an increased shaping gain due to the higher fraction of shaped symbols. For example, consider the first TS scheme. In order to operate at $R_{TX} = 0.25$ bpcu as in Fig. 3 (a), instead of $R_C = 0.5$ we may use $R_C = 0.75$ with p_1 directly given by (5). In the following, we discuss the choice of the code rate for a desired transmission rate.

E. Signaling for a Fixed Transmission and FEC Code Rate

As pointed out in Sec. IV-A, for a target transmission rate R_{TX} and fixed code rate R_C , the probability p_1 is directly given by (5). Thus, for the first TS scheme, the average power constraint in (8) determines A and there are no additional degrees of freedom for the optimization in (9). The second TS scheme has an additional degree of freedom by optimizing over either A_S or A_U .

A practical communication scheme usually uses of a family of channel codes of different rates. For any target transmission rate we are interested in choosing the code rate to minimize the required E_s/N_0 . We proceed as follows.

- 1) Consider a set \mathcal{R}_C of code rates.
- 2) For a target R_{TX} , determine the E_s/N_0 for all possible $R_C \in \mathcal{R}_C$, such that $R_{TX} = R_{TS_i}^*$, $i \in \{1, 2\}$. Since R_{TX} is fixed, for a certain R_C the pulse probability p_1 is obtained from (5).
- 3) Among all $R_C \in \mathcal{R}_C$ use the code rate R_C^* that requires the smallest E_s/N_0 .

As an example, consider the set of code rates $\mathcal{R}_C = \{0.25, 0.33, 0.5, 0.67, 0.75, 0.8, 0.9\}$. For different transmission rates in the range $0.2 \text{ bpcu} \leq R_{TX} \leq 0.85 \text{ bpcu}$ we determine the required E_s/N_0 for the code rates in \mathcal{R}_C , and choose for each R_{TX} the code rate R_C^* with the lowest E_s/N_0 requirement. Table I gives an overview of the code rates R_C^* for some R_{TX} . The gray curves in Fig. 4 represent the corresponding achievable rates versus E_s/N_0 for the first and second TS schemes using code rates from Tab. I. Observe from the table that for the second TS scheme it is beneficial to use high code rates, even if low transmission rates are targeted.

V. PROTOGRAPH-BASED LDPC CODE DESIGN

We now discuss the design of P-LDPC codes [19] for the scheme discussed in Fig. 2. Protographs are small bipartite graphs which serve as a template for a larger LDPC code [19]. A protograph can be represented by an $M \times N$ basematrix \mathbf{B}

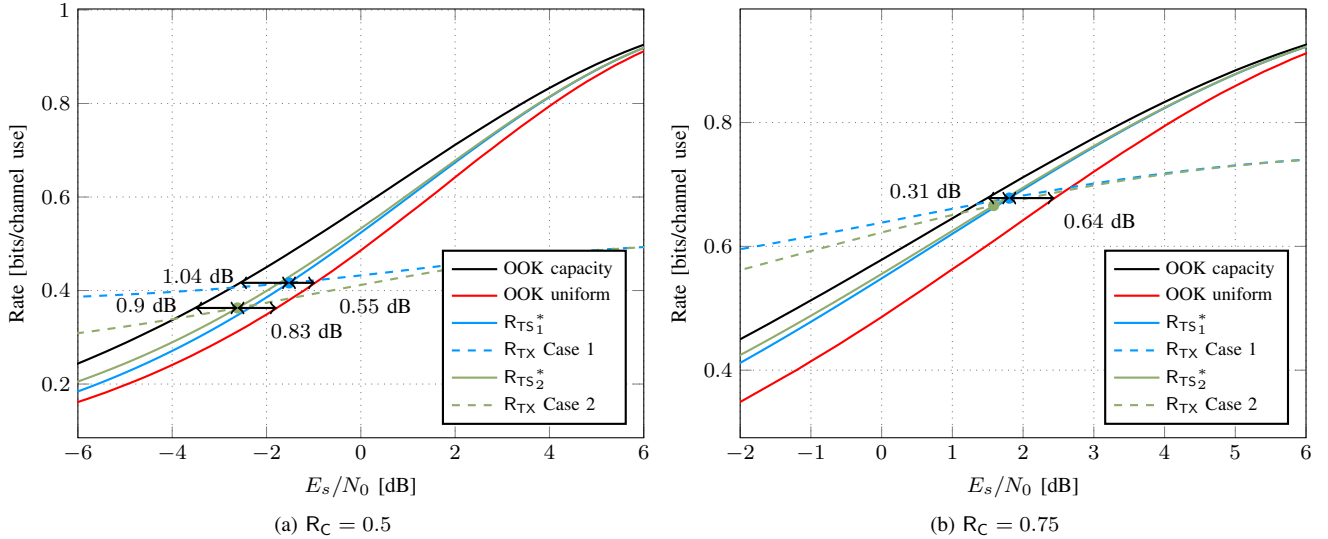


Fig. 3. Achievable rates for the TS scheme with different code rates R_C .

TABLE I
CODE RATES R_C^* FOR SOME R_{TX} .

R_{TX}	R_C^* case 1	R_C^* case 2
0.2	0.33	0.67
0.25	0.5	0.67
0.33	0.5	0.67
0.5	0.67	0.67
0.67	0.75	0.8
0.75	0.8	0.8
0.85	0.9	0.9

which contains elements from \mathbb{N}_0 . An element $b_{i,j}$ indicates the number of parallel edges between a variable node (VN) V_j and a check node (CN) C_i .

The LDPC code is obtained by a copy and permute operations applied to the Tanner graph of the protograph.

We use P-EXIT analysis to determine the decoding threshold of a protograph ensemble [20], [21]. The decoding threshold is the smallest E_s/N_0 such that the probability of symbol error vanishes as the blocklength (as well as the number of decoding iterations) goes to infinity. To briefly describe the algorithm, during each decoding iteration the mutual information between a message at each VN/CN output and the corresponding codeword bit is tracked. The analysis assumes that the messages are Gaussian distributed and that they fulfill the consistency condition [22]. This implies that the mean μ_m and the variance σ_m^2 of the messages are related to each other as $\mu_m = \sigma_m^2/2$.

A. Surrogate Channel Design

For our setting, the decoder soft-information does not fulfill the consistency condition, which is needed for the all-zero codeword assumption and the analysis by P-EXIT. Evaluating (6) for our AWGN model, we obtain

$$L = \underbrace{\frac{A}{\sigma^2} y - \frac{A^2}{2\sigma^2}}_{\text{channel LLR}} + \underbrace{\log \left(\frac{P_X(A)}{P_X(0)} \right)}_{\text{prior}}.$$

The prior for the information symbols breaks the consistency condition. Observe that y is a realization of a Gaussian random variable (RV) with mean $\mu \in \{0, A\}$ and variance σ^2 . Thus, also the L -value is a realization of a Gaussian RV with mean $\left(\pm \frac{A}{2\sigma^2} + \log \frac{P_X(A)}{P_X(0)} \right)$ and variance $\frac{A^2}{\sigma^2}$.

As a workaround, we use a surrogate channel approach [23], i.e., the code is evaluated and optimized for a channel which is different from the target one, but captures its characteristics.

Following [14], we use an AWGN channel with uniformly distributed inputs. We have $\tilde{Y} = \tilde{X} + \tilde{N}$ with $\tilde{X} \in \{0, A\}$ and $\tilde{N} \sim \mathcal{N}(0, \tilde{\sigma}^2)$ as a surrogate and establish equivalence between the surrogate and target channel by requiring

$$H(\tilde{X}|\tilde{Y}) = H(X_S|Y_S). \quad (11)$$

B. EXIT Analysis for the Time Sharing Schemes

In order to perform protograph EXIT analysis we consider the following setup: the first $R_C N$ VNs are connected to a binary-input AWGN surrogate channel with variance $\tilde{\sigma}_S^2$ as described previously. The remaining $(1 - R_C)N$ VNs are connected to a binary-input AWGN channel with variance σ_U^2 . The following modifications with respect to standard P-EXIT analysis are required:

- 1) Pick a target transmission rate R_{TX} and determine the additional parameters (code rate R_C , pulse probability and amplitudes A_S and A_U) as explained in Sec. IV-E. The code rate guides the selection of the protograph dimensions N and M .

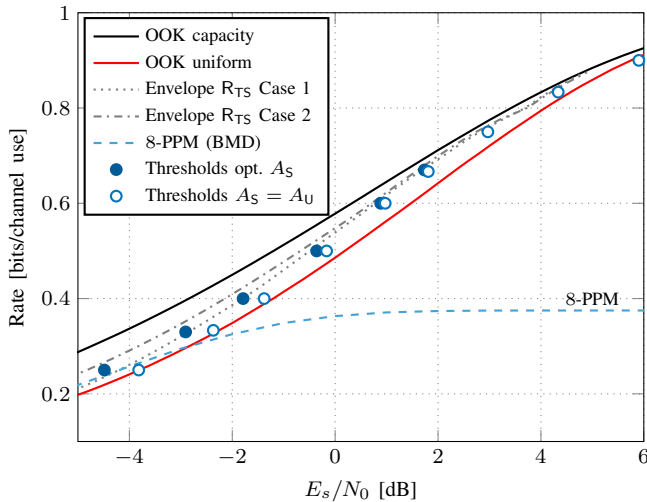


Fig. 4. Achievable rates and thresholds versus E_s/N_0 for various protographs.

- 2) For a $E_s/N_0 = 1/(2\sigma^2)$, compute the corresponding noise variances σ_S^2 and σ_U^2 as

$$\sigma_S^2 = \frac{\sigma^2}{A_{S\text{P}1}^2} \quad \text{and} \quad \sigma_U^2 = \frac{2\sigma^2}{A_U^2}.$$

- 3) For the AWGN channel with variance σ_S^2 , find a surrogate channel with conditional entropy fulfilling (11). Denote the variance of this channel by $\tilde{\sigma}_S^2$.
- 4) Initialize the channel noise variances of the first $R_C N$ VNs of the protograph with $\tilde{\sigma}_S^2$ and of the last $(1-R_C)N$ VNs with σ_U^2 .
- 5) For the target E_s/N_0 , determine the a posteriori mutual information at the protograph VNs (after a sufficiently large number of iterations) by standard protograph EXIT analysis as described in [21].

In order to obtain the iterative decoding threshold of a protograph code ensemble, the above procedure is repeated for different E_s/N_0 . The lowest E_s/N_0 , for which the a posteriori mutual information approaches one for all VNs is the iterative decoding threshold of the protograph ensemble.

C. Protograph Search

To find good protograph ensembles, we use differential evolution (DE) [24]. DE is a genetic optimization algorithm that finds capacity approaching protograph ensembles for various settings. We allow for a maximum number of $M-1$ VNs of degree 2 [25] and set the highest base matrix entry to 4.

VI. NUMERICAL RESULTS

A. Asymptotic Results

We present the decoding thresholds for optimized protograph ensembles in Fig. 4. For the TS scheme one, we consider $R_C \in \{0.5, 0.67, 0.75, 0.8, 0.9\}$. For the TS scheme two, we found optimized codes for $R_C \in \{0.67, 0.8\}$. A comparison to

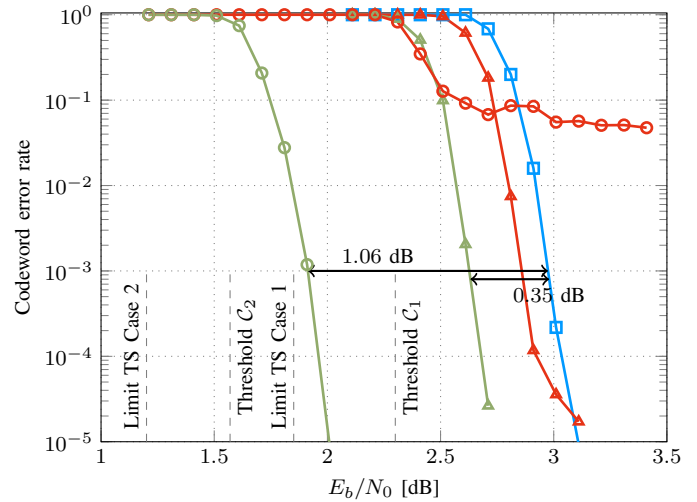


Fig. 5. CER versus E_b/N_0 for $R_{TX} = 0.25$ bpcu. The uniform reference (\square) uses a DVB-S2 code of rate $R_C = 0.25$. For TS Case 1, the optimized code (\blacktriangle) and the DVB-S2 code (\blacktriangleright) code have $R_C = 0.5$. For TS Case 2 we have $R_C = 0.67$ for the optimized (\ominus) and the DVB-S2 LDPC code (\circ).

the achievable rates from Sec. IV-E shows that the thresholds are close to the limits. At $R_{TX} = 0.25$, we obtain a threshold of -3.82 dB for TS scheme one. For the TS scheme two, the threshold is decreased to -4.49 dB. The gaps to the achievable rates are 0.25 dB and 0.3 dB, respectively.

Note that for transmission rates $0.4 < R_{TX} < 0.85$ bits/channel use, TS scheme one has a significant advantage with respect to uniform signaling and PPM with BMD. For $R_{TX} < 0.5$ bits/channel use, TS scheme two gains with respect to PPM with BMD, uniform signaling and TS scheme one. At $R_{TX} = 0.25$, the protograph thresholds of TS scheme two gain 0.67 dB of TS scheme two over TS scheme one.

B. Simulation Results

To verify our asymptotic findings, we construct finite length codes and compare to state-of-the-art off-the-shelf codes. Fig. 5 shows the codeword error rate (CER) versus E_b/N_0 for two different P-LDPC codes with $R_C = 0.5$ (C_1) and $R_C = 0.67$ (C_2) with a block length of $n = 64800$ bits and for a transmission rate of $R_{TX} = 0.25$ bpcu. For $R_C = 0.5$ we consider TS scheme one while for $R_C = 0.67$ we use TS scheme two. For comparison, the performance of an off-the-shelf DVB-S2 code [15] with uniform signaling with $R_C = 0.25$ is shown. Also, the performance of two off-the-shelf DVB-S2 codes with shaping (i.e., for $R_C = 0.5$ and $R_C = 0.67$) is shown. We observe that in the waterfall region shaping gains 0.1 dB for case 1 and 0.35 dB for case 2, using codes from the DVB-S2 standard. However, the DVB-S2 LDPC codes show visible error floors. Our designs gain 0.35 dB for case 1 and 1.1 dB for case 2, respectively.

Fig. 6 depicts the scenario for $R_{TX} = 0.67$ bpcu and TS scheme one. Here we did not consider TS scheme two, since the achievable rate curves in Fig. 4 suggest only small gains.

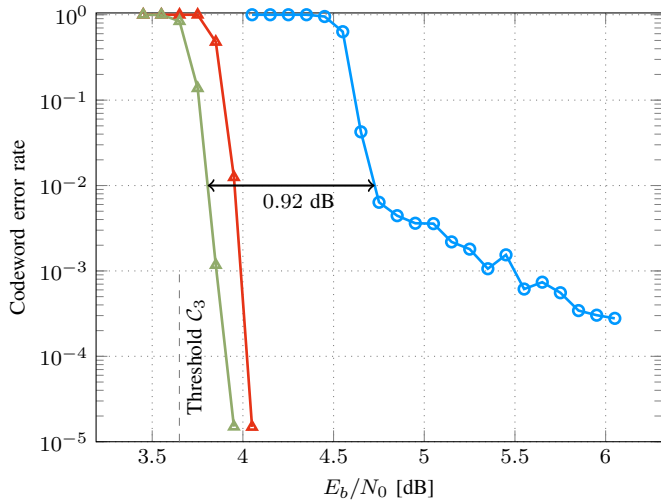


Fig. 6. CER versus E_b/N_0 for $R_{TX} = 0.67$ bpcu. The uniform reference ($\text{---}\circ\text{---}$) uses a DVB-S2 code of rate $R_C = 0.67$. For TS Case 1, the optimized code ($\text{---}\triangle\text{---}$) and the DVB-S2 code ($\text{---}\blacktriangle\text{---}$) code have $R_C = 0.75$.

Let $n = 64800$ and $R_C = 0.75$ for C_3 . With shaping, the Digital Video Broadcasting - Satellite 2 (DVB-S2) code of $R_C = 0.75$ gains 0.8 dB with respect to a DVB-S2 code of $R_C = 0.67$ with uniform signaling. A dedicated P-LDPC code shows gains 0.9 dB with respect to the uniform case.

VII. CONCLUSIONS

We proposed a PS technique for OOK modulated AWGN channels. We design P-LDPC codes using a surrogate AWGN channel approach. The proposed PS scheme outperforms standard OOK with a uniform distribution by 0.7 dB at a transmission rate of 0.25 bpcu if the parity and information OOK symbols are constrained to have the same pulse amplitude. Different amplitudes gain 1.1 dB at a transmission rate of 0.25 bpcu.

ACKNOWLEDGMENT

The authors would like to thank Gerhard Kramer for his valuable comments on this work.

APPENDIX A

BASE MATRICES OF THE SIMULATED CODES

In the following, we provide the optimized base matrices B_1 , B_2 and B_3 for code C_1 , C_2 and C_3 , respectively. For B_1 the first column is punctured.

$$B_1 = \begin{pmatrix} 3 & 0 & 0 & 1 & 2 & 0 & 0 \\ 1 & 0 & 2 & 0 & 0 & 1 & 2 \\ 3 & 0 & 1 & 2 & 2 & 1 & 1 \\ 2 & 1 & 0 & 0 & 0 & 0 & 0 \end{pmatrix} \quad B_2 = \begin{pmatrix} 1 & 0 & 1 & 0 & 2 & 0 & 0 & 0 & 3 \\ 4 & 2 & 3 & 2 & 4 & 2 & 1 & 1 & 3 \\ 3 & 1 & 4 & 1 & 1 & 1 & 2 & 1 & 1 \end{pmatrix}$$

$$B_3 = \begin{pmatrix} 4 & 0 & 1 & 4 & 0 & 3 & 0 & 0 & 2 & 0 & 0 & 0 \\ 0 & 1 & 2 & 3 & 1 & 1 & 1 & 2 & 2 & 1 & 3 & 2 \\ 3 & 2 & 1 & 4 & 1 & 2 & 2 & 1 & 2 & 1 & 1 & 1 \end{pmatrix}$$

REFERENCES

- [1] M. A. Khalighi and M. Uysal, "Survey on free space optical communication: A communication theory perspective," *IEEE Commun. Surveys Tuts.*, vol. 16, no. 4, pp. 2231–2258, 2014.
- [2] B. Moision and J. Hamkins, "Coded modulation for the deep-space optical channel: Serially concatenated pulse-position modulation," Caltech, Pasadena, CA, USA, IPN Progress Report 42–161, May 2005.
- [3] H. Hemmati, A. Biswas, and I. B. Djordjevic, "Deep-space optical communications: Future perspectives and applications," *Proc. IEEE*, vol. 99, no. 11, pp. 2020–2039, 2011.
- [4] *Optical high data rate (HDR) Communication 1550 nm*, Orange Book, Issue 0, Consultative Committee for Space Data Systems (CCSDS) Proposed draft experimental specification 000.0-O-0, Oct. 2018.
- [5] F. Gray, "Pulse code communication," U. S. Patent 2632 058, 1953.
- [6] R. Herzog, A. Schmidbauer, and J. Hagenauer, "Iterative decoding and despreading improves CDMA-systems using M-ary orthogonal modulation and FEC," in *IEEE Int. Conf. Commun. (ICC)*, vol. 2, Jun. 1997, pp. 909–913.
- [7] R. G. Gallager, *Information Theory and Reliable Communication*. John Wiley & Sons, Inc., 1968.
- [8] G. D. Forney, "Trellis shaping," *IEEE Trans. Inf. Theory*, vol. 38, no. 2, pp. 281–300, Mar. 1992.
- [9] G. Forney, R. Gallager, G. Lang, F. Longstaff, and S. Qureshi, "Efficient Modulation for Band-Limited Channels," *IEEE J. Sel. Areas Commun.*, vol. 2, no. 5, pp. 632–647, Sep. 1984.
- [10] W. G. Bliss, "Circuitry for performing error correction calculations on baseband encoded data to eliminate error propagation," *IBM Tech. Disc. Bull.*, vol. 23, pp. 4633–4634, 1981.
- [11] E. Ratzler, "Error-correction on non-standard communication channels," Ph.D. dissertation, University of Cambridge, 2013.
- [12] J. J. Boutros, F. Jardel, and C. Méasson, "Probabilistic shaping and non-binary codes," in *IEEE Int. Symp. Inf. Theory*, Jun. 2017, pp. 2308–2312.
- [13] A. Buchberger, A. Graell i Amat, V. Aref, and L. Schmalen, "Probabilistic eigenvalue shaping for nonlinear fourier transform transmission," *J. Lightw. Technol.*, vol. 36, no. 20, pp. 4799–4807, Oct. 2018.
- [14] F. Steiner, G. Böcherer, and G. Liva, "Protograph-based LDPC code design for shaped bit-metric decoding," *IEEE J. Sel. Areas Commun.*, vol. 34, no. 2, pp. 397–407, 2016.
- [15] "Digital Video Broadcasting (DVB); 2nd Generation Framing Structure, Channel Coding and Modulation Systems for Broadcasting, Interactive Services, News Gathering and Other Broadband Satellite Applications (DVB-S2)," no. EN 302 307, 2009.
- [16] G. Böcherer, F. Steiner, and P. Schulte, "Bandwidth efficient and rate-matched low-density parity-check coded modulation," *IEEE Trans. Commun.*, vol. 63, no. 12, pp. 4651–4665, 2015.
- [17] G. Böcherer, "Capacity-achieving probabilistic shaping for noisy and noiseless channels," Ph.D. dissertation, RWTH Aachen University, 2012. [Online]. Available: <http://www.georg-boecherer.de/capacityAchievingShaping.pdf>
- [18] P. Schulte and G. Böcherer, "Constant composition distribution matching," *IEEE Trans. Inf. Theory*, vol. 62, no. 1, pp. 430–434, 2016.
- [19] J. Thorpe, "Low-density parity-check (LDPC) codes constructed from protographs," *IPN progress report*, vol. 42, no. 154, pp. 42–154, 2003.
- [20] S. Ten Brink, "Convergence of iterative decoding," *Electronics letters*, vol. 35, no. 10, pp. 806–808, 1999.
- [21] G. Liva and M. Chiani, "Protograph LDPC codes design based on EXIT analysis," in *Proc. IEEE Global Telecommun. Conf.*, Washington, DC, USA, Nov. 2007, pp. 3250–3254.
- [22] T. J. Richardson, M. A. Shokrollahi, and R. L. Urbanke, "Design of capacity-approaching irregular low-density parity-check codes," *IEEE Trans. Inf. Theory*, vol. 47, no. 2, pp. 619–637, Feb. 2001.
- [23] F. Peng, W. E. Ryan, and R. D. Wesel, "Surrogate-channel design of universal LDPC codes," *IEEE Commun. Lett.*, vol. 10, no. 6, pp. 480–482, 2006.
- [24] H. Uchikawa, "Design of non-precoded protograph-based LDPC codes," in *IEEE Int. Symp. Inf. Theory*, Honolulu, HI, USA, Jun. 2014, pp. 2779–2783.
- [25] D. Divsalar, S. Dolinar, C. R. Jones, and K. Andrews, "Capacity-approaching protograph codes," *IEEE Journal on Selected Areas in Communications*, vol. 27, no. 6, pp. 876–888, Aug. 2009.